

# Suppression of Superconductivity in Disordered Films: Interplay of Two-Dimensional Diffusion and Three-Dimensional Ballistics<sup>1</sup>

D. S. Antonenko<sup>a, b, c, \*</sup> and M. A. Skvortsov<sup>a, b, \*\*</sup>

<sup>a</sup> Skolkovo Institute of Science and Technology, Moscow, 121205 Russia

<sup>b</sup> Landau Institute for Theoretical Physics, Russian Academy of Sciences, Chernogolovka, Moscow region, 142432 Russia

<sup>c</sup> Moscow Institute of Physics and Technology (National Research University), Dolgoprudnyi, Moscow region, 141700 Russia

\*e-mail: antonenko@itp.ac.ru

\*\*e-mail: skvor@itp.ac.ru

Received September 3, 2020; revised September 8, 2020; accepted September 8, 2020

Suppression of the critical temperature in homogeneously disordered superconducting films is a consequence of the disorder-induced enhancement of Coulomb repulsion. We demonstrate that for the majority of thin films studied now this effect cannot be completely explained under the assumption of two-dimensional diffusive nature of electron motion. The main contribution to the suppression of  $T_c$  arises from the correction to the electron–electron interaction constant coming from small scales of the order of the Fermi wavelength that leads to the critical temperature shift  $\delta T_c/T_{c0} \sim -1/k_F l$ , where  $k_F$  is the Fermi momentum and  $l$  is the mean free path. Thus almost for all superconducting films that follow the fermionic scenario of  $T_c$  suppression with decreasing the film thickness, this effect is caused by the proximity to the three-dimensional Anderson localization threshold and is controlled by the parameter  $k_F l$  rather than the sheet resistance of the film.

DOI: 10.1134/S0021364020190017

## 1. INTRODUCTION

The principal characteristics of a superconductor is its transition temperature  $T_c$ . It is usually assumed that  $T_c$  is a material property and does not depend on the sample size. However, there is a strong experimental evidence of the systematic decrease in the critical temperature in disordered superconducting films with decreasing its thickness,  $d$  (V [1], NbN [2–9], TiN [10], MoGe [11, 12], MoSi [13, 14], MoC [15], WRe [16], InO [17], etc. [18]). The suppression of  $T_c$  becomes pronounced typically at  $d \sim 10$  nm, and for the thinnest films  $T_c$  may eventually vanish, marking the point of a quantum superconductor–metal or superconductor–insulator transition [19–24].

Depending on the underlying structure of a material, two scenarios of suppression of  $T_c$ , fermionic and bosonic, have been identified. The bosonic scenario applies to granular and/or strongly inhomogeneous superconductors with localized preformed Cooper pairs (polycrystalline TiN, amorphous InO) [25–28], where  $T_c$  signals proliferation of superconducting coherence from micro- to macro-scales. In the fermi-

onic scenario, relevant for structureless homogeneously disordered superconductors (NbN, MoGe, etc.), suppression of superconductivity is a consequence of the disorder-induced enhancement of electron repulsion [29, 30], which leads to the decrease in the effective Cooper pairing constant. Despite the common physical mechanism of disorder-induced  $T_c$  suppression in the fermionic scenario, its description for three- and two-dimensional systems is rather different.

In the three-dimensional (3D) geometry, enhancement of repulsion due to scattering off the impurity potential is provided by small distances, not exceeding the mean free path  $l$ . As a result, the whole effect can be completely described by the change in the Cooper pairing constant. The fermionic mechanism for strongly disordered 3D superconductors near the Anderson localization threshold ( $k_F l \sim 1$ , where  $k_F$  is the Fermi momentum) was studied by Anderson, Muttalib, and Ramakrishnan [31]. They also estimated the correction to the bare electron–electron interaction constant  $\lambda$  in the case of weak disorder ( $k_F l \gg 1$ ):  $\delta\lambda/\lambda \sim 1/(k_F l)^2$ . Similar expressions were reported in [32, 33]. This estimate can be easily obtained by cutting the 3D diffusive contribution at

<sup>1</sup> Supplementary materials are available for this article at <https://doi.org/10.1134/S0021364020190017> and are accessible for authorized users.

the ultraviolet cutoff  $r \sim l$ . However, as shown by Belitz and Kirkpatrick in their study of weak-localization correction to the conductivity [34, 35], diffusive contributions in the 3D geometry are extended to the ballistic region up to the distances of the order of wavelength and have a relative order of  $1/(k_F l)$  rather than  $1/(k_F l)^2$ . Similar phenomenon of extension of interaction-induced contribution from the diffusive to the ballistic region is also known for the tunneling density of states, both in two-dimensional [36] and three-dimensional geometries [37, 38].

Disorder-induced renormalization of the electron–phonon interaction and its impact on superconductivity were studied by Keck and Schmid [39]. They showed that the displacement of impurities by the lattice vibrations leads to the suppression of the interaction with longitudinal phonons and the emergence of the interaction with transverse phonons. An attempt to account for the impurity corrections both to the Coulomb and electron–phonon interactions and their influence on  $T_c$  was taken by Belitz with the help of the exact-eigenstates technique [40] and by solving full Gor’kov equations in the strong-coupling regime [41–43]. A part of his results can be interpreted as a correction to the bare electron–electron coupling constant  $\delta\lambda/\lambda \sim 1/k_F l$ . However, Belitz’s results were called into question by Finkel’stein [44] by demonstrating that elastic diagrams, intimately related to the correction to the tunneling density of states [45, 46] and claimed to be essential by Belitz, actually do not contribute to the  $T_c$  shift in the leading order.

The main difference of the *two-dimensional (2D) geometry* compared to the 3D case is that the renormalization effect does not boil down to the energy-independent shift of the coupling constant  $\lambda$  and requires a summation of the leading logarithms. Conventional description of  $T_c$  suppression in thin superconducting films substantially relies on *2D diffusive* nature of electron motion, which is motivated by the experimentally relevant hierarchy of length scales  $\lambda_F \ll l \ll d \ll \xi_0$  (see Fig. 1). (Here,  $\lambda_F$  is the Fermi wavelength,  $\xi_0 = \sqrt{\hbar D/T_c}$  is the superconducting coherence length in the dirty limit, and  $D$  is the diffusion constant.) In this paradigm, enhancement of disorder with the decrease in the film thickness  $d$  is related to the increase in the sheet resistance of the film,  $R_{\square}$ .

The effect of  $T_c$  shift due to the interplay of disorder and interaction was studied on a perturbative level in [45–49], where the 2D diffusive contribution to the  $T_c$  shift was calculated:

$$\frac{\delta T_c}{T_{c0}} = -\frac{\lambda}{3\pi g} \log^3 \frac{\hbar}{T_{c0} \tau_*}, \quad (1)$$

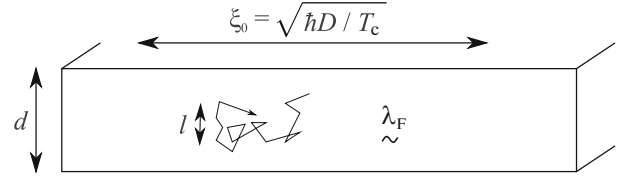


Fig. 1. Experimentally relevant hierarchy of length scales in disordered superconducting films.

where  $T_{c0}$  is the critical temperature of a bulk superconductor,  $g = h/e^2 R_{\square} = (2/3\pi)(k_F l)(k_F d) \gg 1$  is the dimensionless film conductance, and  $\lambda$  is the dimensionless coupling constant of the electron–electron interaction (for the screened Coulomb interaction,  $\lambda = 1/2$ ). The parameter  $\tau_*$  is the time when diffusion becomes two-dimensional:  $\tau_* = \max\{\tau, \tau_d\}$ , where  $\tau$  is the elastic scattering time and  $\tau_d = d^2/4D$  is the time of diffusion across the film thickness [44, 47]. In real space, the logarithm in Eq. (1) is accumulated from the 2D diffusion from the length scale  $\max(l, d)$  to the coherence length  $\xi_0$ . The correction (1), inversely proportional to the film conductance, is conceptually similar to the weak-localization [50, 51] and interaction-related [30] corrections to the 2D conductivity, while two out of three powers of the logarithm are due to the exponential sensitivity of  $T_c$  to the coupling constant  $\lambda_{\text{BCS}}$ .

The first-order perturbative result (1) has later been generalized to the case of arbitrarily strong  $T_c$  suppression by Finkel’stein, who managed to sum the leading logarithms with the help of the renormalization-group technique [44, 52]. The same result can be obtained by solving the self-consistency equation with an energy-dependent Cooper coupling  $\lambda_{E,E'} = \lambda_{\text{BCS}} - \gamma_g^2 \log[1/\max(E, E')\tau_*]$  [53]. For the screened Coulomb interaction ( $\lambda = 1/2$ ), the nonperturbative expression for the critical temperature as a function of the dimensionless film conductance valid until superconductivity is fully suppressed is given by:

$$\log \frac{T_c}{T_{c0}} = \frac{1}{\gamma} - \frac{1}{2\gamma_g} \log \frac{\gamma + \gamma_g}{\gamma - \gamma_g}, \quad (2)$$

where  $\gamma_g = 1/\sqrt{2\pi g}$  and  $\gamma = 1/\log(\hbar/T_{c0}\tau_*)$ . Expression (2), where  $\gamma$  is considered as a fitting parameter, was used by Finkel’stein [44] to explain the observed dependence of  $T_c$  in MoGe films [11] on the film thickness, the latter being directly related to the dimensionless conductance  $g$ . Since then, such an explanation of experimental data on superconductivity suppression in disordered films has become generally accepted [14, 15, 54].

**Table 1.** Parameters of superconducting films\*: bulk critical temperature  $T_{c0}$ , thickness  $d$ , mean free path  $l$ , the value of  $\gamma$  obtained from fitting  $T_c(g)$  dependence with Eq. (2) and the values of the two logarithms:  $\mathcal{L} = \log(\hbar/T_{c0}\tau)$  and  $\mathcal{L}_d = \log(\hbar/T_{c0}\tau_d)$

Material	Ref.	$T_{c0}$ , K	$d$ , nm	$l$ , Å	$\gamma_{\text{fit}}^{-1}$	$\mathcal{L}$	$\mathcal{L}_d$
NbN	[4]	15	2–15	~5	5.0	5.7	5.6–3.4
NbN	[5]	15	1–26	2	8.3	7.2	6.2–2.1
NbN	[8]	17	>50	<7	–	4.8	3D
TiN	[10]	5	3.6–5	3	6.2	8.9	6.4–2.4
MoGe	[11, 52]	7	1.5–100	~4	8.2	6	<4.0
MoSi	[13]	7	1–20	5	7.0	5.6	<4.7
MoC	[15]	8	3–30	<4	7.5	5.5	3.2–0.9
WRe	[16]	6	3–120	4	7.4	6.1	<2.7
Nb	[58]	7	2.5–26	18	11.7	5.2	<4.8

\*For WRe and TiN films, we took  $l/k_F \sim l \sim a$ , where  $a$  is the interatomic distance. For MoC films, the free electron mass was taken for the effective mass.

According to Eqs. (1) and (2),  $T_c$  suppression in thin ( $d \ll \xi_0$ ) superconducting films is entirely determined by the dimensionless sheet conductance  $g$ . Such a statement perfectly fits the general theoretical framework of scaling [50], justified by the renormalization-group analysis of the nonlinear sigma model in the 2D space [55–57].

However, interpretation of experimental data on  $T_c(d)$  dependence with the help of Eq. (2) encounters a number of significant difficulties. The first one is the internal inconsistency of the approach that treats  $\gamma$  as a free fitting parameter. As follows from Table 1, which contains experimental data on different films, the values of  $\gamma_{\text{fit}}^{-1}$  obtained by fitting  $T_c(d)$  dependence with the help of Eq. (2) typically lie in the interval of 7–9. The issue is that these values significantly exceed the theoretical estimate  $\gamma^{-1} = \mathcal{L}_d = \ln(\hbar/T\tau_d)$  (last column in Table 1), and in half of the cases exceed even the quantity  $\mathcal{L} = \ln(\hbar/T\tau)$  (last but one column in Table 1). Taking into account that the perturbative shift of  $T_c$ , according to Eq. (1), is proportional to the third power of this logarithm, one can conclude that the discrepancy between the microscopic theory and the result of the fit with Eq. (2) appears to be very large. One can try to save the situation by pointing to the fact that  $\gamma_{\text{fit}}^{-1}$  should also contain the contribution of 3D diffusion, but that makes the usage of Eqs. (1) and (2) dubious as they were obtained under the assumption of 2D diffusion.

Another problem with interpreting experimental data in terms of Eq. (2) is an implicit assumption that the effect of  $T_c$  suppression is determined by the dimensionless film conductance only. However, in real thin films, the impurity concentration and hence the mean free path  $l$  do vary with the film thickness

due to peculiarities of the fabrication process. Large amount of experimental data on the critical temperature of thin films was analyzed in [59], where it was demonstrated that  $T_c$  is primarily dependent on the 3D bulk conductivity  $\sigma \propto k_F^2 l$  rather than the 2D sheet conductance  $g \propto k_F^2 l d$ .

Inapplicability of Eq. (2) for the description of  $T_c$  suppression in thin films is actually a consequence of (i) too narrow interval of 2D diffusion (from  $d$  to  $\xi_0$ ), which appears to be insufficient to explain the observed magnitude of the effect and (ii) the smallness of the prefactor  $1/g \sim (k_F l)^{-1} (k_F d)^{-1}$ . Hence, for a quantitative description of experimental data, one has to specify another mechanism of disorder-induced enhancement of the Coulomb interaction that is not related to 2D diffusion.

In this work, we demonstrate that existing experimental data on  $T_c$  suppression in thin films can be convincingly explained assuming that the main contribution stems from the processes of *three-dimensional ballistic* motion of electrons with a typical distance between the interaction point and the point of impurity scattering of the order of several wavelengths. Our main result is the amendment of the perturbative expression (1) for  $T_c$  shift:

$$\frac{\delta T_c}{T_{c0}} = -\frac{\alpha}{k_F l} - \frac{\lambda}{3\pi g} \log^3 \frac{\hbar}{T_{c0} \tau_d}, \quad (3)$$

where the added first term accounts for the contribution of the 3D ballistic region. We emphasize that since all scales starting from the Fermi wavelengths contribute to  $T_c$  suppression, keeping the last term originating from the 2D diffusion region on the background of the first one may be justified only for mate-

rials with exceptionally low  $T_c$  or very small thickness (in particular, for atomically thin films [60]).

The coefficient  $\alpha$  in Eq. (3) is nonuniversal and depends on the details of the interaction and the structure of the random potential. In the model of weak short-range electron repulsion (amplitude  $\lambda$ ) and Gaussian white-noise random potential, it is given by

$$\alpha = \frac{\pi\lambda \log^2 \omega_D/T_c}{2(1 + \lambda \log E_F/\omega_D)^2}. \quad (4)$$

For realistic superconducting films with the Coulomb interaction one should expect a material dependent value  $\alpha \sim 1$ .

## 2. MODEL

We consider a model of  $s$ -wave superconductivity with a phonon-mediated electron attraction described by the potential  $V_{\text{ph}}(\mathbf{r}) = -(\lambda_{\text{ph}}/v)\delta(\mathbf{r})$  effective in the in the energy strip of  $\omega_D$  near the Fermi energy, and a short-range repulsion with the potential  $V(\mathbf{r}) = (\lambda/v)\delta(\mathbf{r})$  and an energy cutoff at  $E_F$ . We will work in the weak-coupling approximation,  $\lambda_{\text{ph}}, \lambda \ll 1$ , and neglect disorder-induced renormalization of the phonon vertex beyond the ladder approximation [39]. Disorder is modeled by a random potential with the Gaussian white-noise statistics described by the correlator  $\langle U(\mathbf{r})U(\mathbf{r}') \rangle = \delta(\mathbf{r} - \mathbf{r}')/2\pi v\tau$ , where  $v$  is the density of states at the Fermi level (for one spin projection) and  $\tau$  is the elastic scattering time.

In the absence of disorder-induced renormalization of the interaction vertices,  $T_c$  is given by the standard expression of the Bardeen–Cooper–Schrieffer (BCS) theory:

$$T_{c0} = \omega_D \exp(-1/\lambda_{\text{BCS}}), \quad (5)$$

where the effective coupling constant is

$$\lambda_{\text{BCS}} = \lambda_{\text{ph}} - \frac{\lambda}{1 + \lambda \log E_F/\omega_D}. \quad (6)$$

The second term, known as the Tolmachev logarithm in Russia and as the Coulomb pseudopotential in the West, describes the effect of the Coulomb repulsion in the Cooper channel undergoing logarithmic renormalization in the energy window from  $E_F$  to  $\omega_D$  [61–63], see also the supplemental material.

The critical temperature is determined by the pole of the Cooper ladder at zero momentum and frequency in the Matsubara diagrammatic technique. In the presence of a random potential, the diagrammatic series should be averaged over disorder in every possible way. In the leading order (no-crossing approximation), this process reduces to independent averaging of the product of the two Green's functions,  $G_E G_{-E}$ , connecting the interaction vertices ( $\lambda_{\text{ph}}$  or  $\lambda$ ), which is done via insertion of a cooperon. According to the

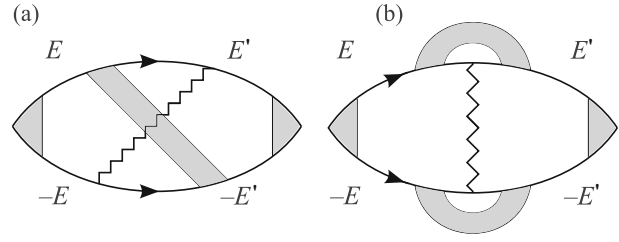


**Fig. 2.** Inelastic diagrams for the diffusive contribution ( $q \ll 1/l$  and  $E, E' \ll 1/\tau$ , where  $q$  is the momentum carried by the interaction line) to the Cooper susceptibility that determine  $T_c$  shift. The shaded blocks in the center of the diagrams are cooperons and diffusons connecting the Green's functions with the opposite Matsubara energy signs. The shaded triangles in the corners of the diagrams designate renormalization of the phonon vertex by the impurity ladders and ladders of electron interaction with the constant  $\lambda$ .

Anderson theorem [64–66], the result is disorder independent and leads to Eqs. (5) and (6) for the critical temperature.

## 3. DIFFUSIVE CONTRIBUTION

In order to find the shift of  $T_c$ , one has to take into account processes describing an interplay of interaction and disorder in the next order with respect to no-crossing diagrams [44–46, 48, 49, 52]. The leading diagrammatic contributions in the diffusive region are shown in Fig. 2, where the interaction (zigzag line) is crossed by the impurity ladders, diffusons and cooperons, depicted as gray blocks. The diagram (a) has a mirrored counterpart, while the diagram (b) contains two additional contributions with an impurity line connecting the Green's functions with the energy of the same sign (Hikami box) [67]. Analytical expression for  $T_c$  shift contains a summation over two Matsubara energies  $E$  and  $E'$  (see the supplemental material):

$$\frac{\delta T_c}{T_{c0}} = -\frac{2\pi\lambda}{v} \left( \frac{\lambda_{\text{ph}}}{\lambda_{\text{BCS}}} \right)^2 T^2 \sum_{E, E' > 0}^{E_F} \frac{u(E)u(E')I_{E, E'}}{EE'}, \quad (7)$$

where the factor  $\lambda_{\text{ph}}/\lambda_{\text{BCS}}$  and the logarithmic function  $u(E) = \theta(\omega_D - E) - (\lambda \log \omega_D/T)/(1 + \lambda \log E_F/T)$  represent renormalization effects, which can be introduced by adding  $\lambda$ -interaction ladders to the left and right vertex of the diagram. In the diffusive region, the quantity  $I_{E, E'}$  in the film geometry can be expressed via an integral over the 2D in-plane momentum  $q_{\parallel}$  and a sum over the transverse modes of the Laplace operator with the Neumann boundary conditions

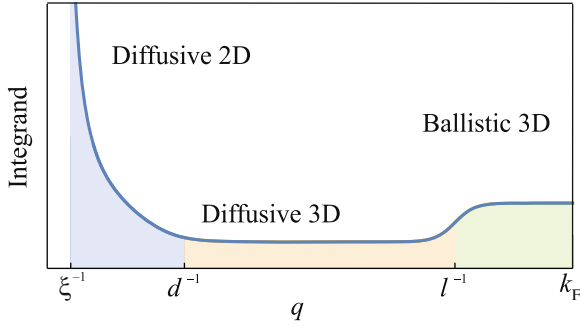


**Fig. 3.** (Color online) Sketch of the dependence of integrand in Eq. (8) on  $q$  (at not too large  $E + E'$ ). In the region  $q > 1/d$  it has a weak  $q$  dependence, changing by a factor of  $\pi^2/8$  at the crossover from the diffusive to ballistic motion (at  $q \sim 1/l$ ).

( $q_z = 2\pi m/d$ , with  $m = 0, 1, \dots$ ) carried by the interaction line (see the supplemental material):

$$I_{E,E'} = \frac{\tau}{d} \sum_{q_z} \int \frac{d\mathbf{q}_{\parallel}}{(2\pi)^2} \frac{f_q(E+E')^2 [3 - f_q(E+E')]}{1 - f_q(E+E')}. \quad (8)$$

To trace the crossover to the ballistic region, we write cooperons and diffusons beyond the diffusive approximation and express them via the function  $f_q(\omega) = (ql)^{-1} \arctan[ql/(1 + |\omega|\tau)]$ , which corresponds to the one step of the impurity ladder at arbitrary values of  $ql$  and  $\omega\tau$ , but under the conditions  $q \ll k_F$  and  $\omega \ll E_F$ . An analogous approach was used in [68] to calculate the fluctuation conductivity at arbitrary disorder strength.

The leading 2D diffusive contribution stems from the mode with  $q_z = 0$ . Cutting the integral over  $q$  at the momentum  $1/d$  and the energy summation at  $\omega_D$ , and taking into account that for realistic films studied in experiments the Debye frequency  $\omega_D$  is comparable to  $\hbar/\tau_d$  [9], we arrive at the well-known result (1) with  $\tau_* \sim \tau_d$ . Note, however, that the extraction of the 2D diffusive contribution out of expressions (7) and (8) is complicated by the fact that the contributions of other regions are in fact larger. Indeed, at the scale  $q \sim 1/d$  the 2D logarithmic behavior is changed to a linearly divergent one due to excitation of higher transverse modes, making the momentum integral three-dimensional. One can estimate the contribution of the 3D diffusive region by introducing an artificial cutoff at  $q \sim 1/l$ , which gives

$$\frac{\delta T_c^{(\text{diff, 3D})}}{T_{c0}} \sim -\frac{\lambda}{(k_F l)^2} \log^2 \frac{\omega_D}{T_{c0}}. \quad (9)$$

This contribution has only two out of three logarithmic factors but it exceeds Eq. (1) by the parameter  $d/l \gg 1$ . However, nothing prevents considering even

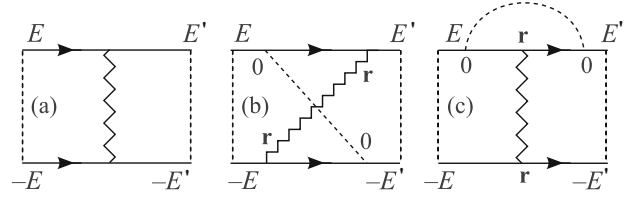


**Fig. 4.** (a) Electron–electron interaction vertex  $\lambda_c$  in the Cooper channel with the first impurity line of the surrounding cooperons. (b, c) Diagrams describing the leading vertex correction  $\delta\lambda_{E,E'}^c$  from the ballistic region. Both diagrams have mirrored counterparts.

greater momenta in Eq. (8) and study the ballistic region  $q \gg 1/l$ . Remarkably, in this region the integrand of Eq. (8) still obeys the  $1/q^2$  behavior, but with a different numerical prefactor. This means that the main contribution to the integral originates from momenta of the order of Fermi momentum,  $q \sim k_F$ . This region requires a special treatment, which will be done below. Schematically, the role of different momentum regions is illustrated in Fig. 3. Up to logarithmic factors coming from the energy summations, the integral of the shown curve determines the contribution of the corresponding regions to  $T_c$  shift.

#### 4. BALLISTIC CONTRIBUTION

In this section, we study the ballistic contribution to  $T_c$  shift originating from processes with the momentum transfer  $q > 1/l$ . Due to the assumption  $l \ll d$ , electron motion can be assumed to be three-dimensional. This contribution is described by the diagrams shown in Fig. 2, where we left only one impurity line out of the diffusive ladder, which corresponds to scattering on one impurity. For an accurate calculation, one should reconsider expression (8), relaxing the assumption  $q \ll k_F$ .

The ballistic contribution can be described as a correction to the bare (unrenormalized) repulsive electron–electron coupling constant in the Cooper channel,  $\lambda^c$ , which in the leading order coincides with  $\lambda$  (Fig. 4a). The leading corrections are given by the diagrams Figs. 4b and 4c. In the considered model of point-like interaction and delta-correlated disorder, the calculation of these diagrams can be performed analytically and leads, generally speaking, to an energy-dependent correction  $\delta\lambda_{E,E'}^c$  to the Cooper-channel coupling:

$$\frac{\delta\lambda_{E,E'}^c}{\lambda} = 2 \frac{(b) + (c)}{(a)} = \frac{2[P(E, E') + P(E, -E')]}{(2\pi\nu\tau)^2 f_0(2E)f_0(2E')\lambda}, \quad (10)$$

where the terms in the brackets correspond to the diagrams (b) and (c), respectively, and the numerical

coefficient 2 is due to mirrored diagrams. The factors  $f_0(\omega) = 1/(1 + |\omega|\tau)$  in the denominator originate from the momentum integration of a pair of the Green's functions in Fig. 4a (one step of the diffusive ladder).

It is convenient to calculate the block  $P(E, E')$  in the coordinate representation [38]. Since the electron–electron interaction as well as the disorder correlator are assumed to be point-like, analytical expression contains only one integral over the distance  $\mathbf{r}$  between the impurity and the interaction point, so we get:

$$P(E, E') = \frac{\lambda}{2\pi\nu\tau} \int d\mathbf{r} G_+ G'_- [G_+ G_-] [G'_+ G'_-], \quad (11)$$

where  $G_{\pm} = G_{\pm E}(\mathbf{r})$  are disorder-averaged Green's functions and the prime refers to the energy argument  $E'$ . The square brackets denote the real-space convolution:  $[G_+ G_-] = \int G_+(\mathbf{p}) G_-(\mathbf{r} - \mathbf{p}) d\mathbf{p}$ . As will be demonstrated below, the integral over  $\mathbf{r}$  in Eq. (11) converges on the scale  $1/k_F$  that allows replacing the Green's functions by their values in the absence of disorder:

$$G_{\pm} = -\pi\nu \frac{e^{\pm ik_F r}}{k_F r}, \quad [G_+ G_-] = \frac{2\pi\nu\tau}{1 + 2|E|\tau} \frac{\sin k_F r}{k_F r}, \quad (12)$$

where the convolution was calculated under the assumption  $E, E' \ll E_F$ .

One can easily show that the integral in Eq. (11) vanishes for different signs of the energies  $E$  and  $E'$ , and thus  $P(E, E') \propto \theta(EE')$ . Thereby in the considered model, the ballistic diagrams in Figs. 4b and 4c are nonzero for the same relation between the energy signs as for the diffusive diagrams in Figs. 2a and 2b, respectively. This conclusion is a priori not obvious because a single impurity line can connect two Green's functions of the same energy sign. However, we see that in the case of the point-like interaction and delta-correlated disorder, these diagrams vanish in the ballistic limit as well.

Substituting Eq. (12) to Eq. (11) and then to Eq. (10), we observe that the factors  $(1 + 2|E|\tau)$  and  $(1 + 2|E'|\tau)$  in the denominators of  $[G_+ G_-]$  and  $[G'_+ G'_-]$  cancel the same factors  $f_0(E)$  and  $f_0(E')$  in Eq. (10). The only energy dependence of  $\delta\lambda_{E, E'}^c$  is thus due to the factor  $\theta(EE')$  contained in the block  $P(E, E')$ . However, it also disappears because of the structure of Eq. (10). As a result, the correction  $\delta\lambda_{E, E'}^c$  appears to be energy-independent:

$$\delta\lambda^c = \frac{\pi\nu\lambda}{2\tau} \int \frac{d\mathbf{r}}{(k_F r)^2} \left( \frac{\sin k_F r}{k_F r} \right)^2 = \frac{\pi\lambda}{2k_F l}. \quad (13)$$

As expected, the integral stems from the scales of the order of the electron wavelength, which is typical for 3D mesoscopic effects [34, 69, 70].

The obtained correction may be interpreted in the spirit of [36] as the renormalization of the contribution of electron–electron interaction to the Cooper channel due to scattering on Friedel oscillations, caused by impurities. This correction describes the enhancement of the electron–electron repulsion, leading to the increase in the Coulomb pseudopotential and, consequently, to the suppression of the effective coupling constant  $\lambda_{\text{BCS}}$ . Suppression of  $T_c$  can be found by substituting  $\lambda$  by  $\lambda + \delta\lambda^c$  and expanding Eq. (6) in  $\delta\lambda^c$ :

$$\frac{\delta T_c^{(\text{ball, 3D})}}{T_{c0}} = -\frac{\pi}{2} \frac{\lambda}{k_F l} \left( \frac{\log \omega_D / T_{c0}}{1 + \lambda \log E_F / \omega_D} \right)^2. \quad (14)$$

## 5. ROLE OF ELASTIC DIAGRAMS

Besides *inelastic* diagrams shown in Figs. 2 and 4, where the interaction line connects the upper and lower Green's functions, there is a set of *elastic* diagrams related to the interaction correction to the one-particle Green's function. As demonstrated by Finkel'stein [44] for 2D diffusion, the contribution of this set of diagrams is always small: at  $Dq^2 > \omega$  they contain a smaller power of a large logarithm, while at  $Dq^2 < \omega$  their contribution is canceled by contributions of inelastic diagrams and of an additional set of diagrams restoring the gauge invariance of the theory. The latter diagrams become subleading already in the diffusive region at  $Dq^2 > \omega$  and therefore are not considered in the present paper.

In the case of an instantaneous electron–electron interaction, there is an exact relation [40, 45, 46] between the contribution of elastic diagrams to  $T_c$  shift and correction to the tunneling density of states  $\delta\nu(\varepsilon)$ , which can be represented in the form analogous to Eq. (7) (see the supplemental material):

$$\frac{\delta T_c^{(\text{elast})}}{T_c} = \left( \frac{\lambda_{\text{ph}}}{\lambda_{\text{BCS}}} \right)^2 T \sum_E \int d\varepsilon \frac{u^2(E)}{E^2 + \varepsilon^2} \frac{\delta\nu(\varepsilon)}{\nu_0}. \quad (15)$$

We will use known results for  $\delta\nu(\varepsilon)$  in order to estimate the contribution (15) of elastic diagrams.

The correction to the tunneling density of states of a 3D metal in the diffusive region ( $|\varepsilon| < 1/\tau$ ) has the form  $\delta\nu_{\text{diff}}(\varepsilon)/\nu_0 \sim \lambda\sqrt{|\varepsilon|\tau}/(k_F l)^2$  [71]. A simple algebra reveals that the contribution to  $T_c$  shift from this region is proportional to  $1/(k_F l)^2$ , which is parametrically smaller than the contribution of the ballistic region discussed below.

The correction to the tunneling density of states in the 3D ballistic region ( $|\varepsilon| > 1/\tau$ ) was studied in [37, 38] and appeared to be linear in energy and generally

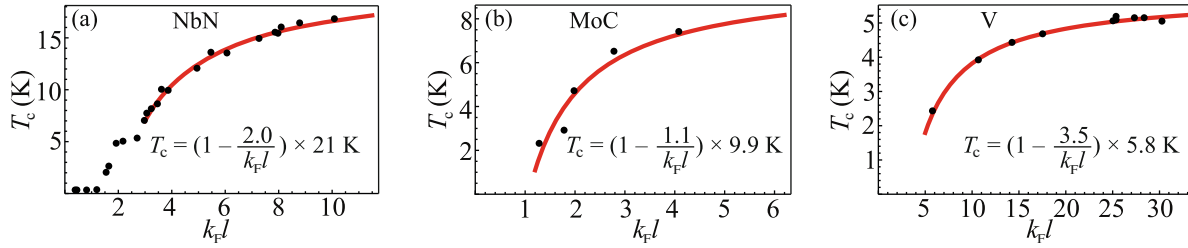


**Fig. 5.** (Color online) Experimental points for the dependence of  $T_c$  on  $k_F l$  and (solid line) their fitting by Eq. (17) for superconducting films of different thicknesses and compositions (a) NbN [8], (b) MoC [15], and (c) V [1].

asymmetric with respect to the Fermi level. In the case of a point-like interaction, delta-correlated disorder, and parabolic electron spectrum, it is finite only for energies below the Fermi energy and has the form  $\delta v_{\text{ball}}(\epsilon)/v_0 \sim \lambda |\epsilon| \theta(-\epsilon)/(k_F l)$  [38]. Then, Eq. (15) yields

$$\frac{\delta T_c^{(\text{ball, 3D, elast})}}{T_{c0}} \sim \frac{\lambda^3}{k_F l} \left( \frac{\log \omega_D/T_{c0}}{1 + \lambda \log E_F/\omega_D} \right)^2, \quad (16)$$

which is parametrically smaller than the leading contribution (14) under the model assumption  $\lambda \ll 1$ . The absence of a linear-in- $\lambda$  contribution from elastic diagrams is related to the fact that, contrary to Eq. (7) with two logarithmic summations over  $E$  and  $E'$ , the integral (15) in the 3D ballistic region is not logarithmic. The conclusion that elastic diagrams do not contribute to the leading  $T_c$  shift is presumably quite general and related to the fact that the tunneling density of states is not a thermodynamic quantity.

## 6. CONCLUSIONS

To summarize, we have studied the influence of the 3D ballistic region of electrons motion on the critical temperature degradation of moderately disordered superconducting films ( $k_F l \gg 1$ ). Within the model of a point-like repulsion and delta-correlated disorder, we have calculated the perturbative contribution of this region to  $T_c$  suppression given by the first term in Eq. (3). When comparing our theory with experimental data, one should take into account that in real samples  $\lambda \sim 1/2$  due to the Coulomb interaction and that the numerical factor in Eq. (4) is model-specific. In general, one might expect that the ballistic contribution to  $T_c$  shift has the form  $\delta T_c/T_{c0} = -\alpha/k_F l$  with  $\alpha \sim 1$ .

The second term in Eq. (3) describes the standard contribution to  $T_c$  suppression originating from the region of two-dimensional electron diffusion, where the logarithm stems from the spatial scales between the film thickness  $d$  and the coherence length  $\xi_0$ . The smallness of this interval for realistic films and a relatively large value of the dimensionless conductance

$g \sim (k_F l)(k_F d)$  makes it practically negligible compared to the three-dimensional ballistic contribution.

Figure 5 presents the fits of experimental data ( $T_c$ ,  $k_F l$ ) for superconducting films of different thicknesses made of three different materials following the fermionic scenario of  $T_c$  suppression by the formula

$$T_c = (1 - \alpha/k_F l)T_{c0}, \quad (17)$$

where  $\alpha$  and  $T_{c0}$  are treated as fitting parameters. A rather good agreement is observed, with the material-dependent value of  $\alpha$  being of the order of one, as expected. We emphasize that the data for NbN presented in Fig. 5a refer to thick films [8], for which there is no two-dimensional diffusive region at all (see Table 1).

Based on (i) the observed agreement between experimental data and Eq. (17), (ii) intrinsic inconsistencies of the theory behind Eq. (2) mentioned above, and (iii) the findings of [59], which indicate that  $T_c$  is primarily dependent on the 3D conductivity rather than the 2D sheet conductance, we make the following practically relevant conclusion:

*For a substantial fraction of not too thin moderately disordered superconducting films that follow the fermionic scenario of superconductivity suppression, the latter is governed by the proximity to the threshold of three-dimensional Anderson localization and controlled by the parameter  $k_F l$ . Two-dimensional diffusion effects, controlled by dimensionless conductance  $g$  are also present, but they typically constitute only a small correction on top of three-dimensional ballistic effects.*

## ACKNOWLEDGMENTS

We are grateful to I.S. Burmistrov, M.V. Feigel'man, A.M. Finkel'stein, P. Samuely, P. Szabó, K.S. Tikhonov, and P.M. Ostrovsky for useful discussions.

## FUNDING

This work was supported by the Russian Science Foundation, project no. 20-12-00361.

## REFERENCES

1. A. A. Teplov, *Sov. Phys. JETP* **44**, 422 (1976).
2. Z. Wang, A. Kawakami, Y. Uzawa, and B. Komiyama, *J. Appl. Phys.* **79**, 7837 (1996).
3. A. Semenov, B. Günther, U. Böttger, H.-W. Hübers, H. Bartolf, A. Engel, A. Schilling, K. Ilin, M. Siegel, R. Schneider, D. Gerthsen, and N. A. Gippius, *Phys. Rev. B* **80**, 054510 (2009).
4. Y. Noat, V. Cherkez, C. Brun, T. Cren, C. Carbillet, F. Debontridder, K. Ilin, M. Siegel, A. Semenov, H.-W. Hübers, and D. Roditchev, *Phys. Rev. B* **88**, 014503 (2013).
5. K. Makise, T. Odou, S. Ezaki, T. Asano, and B. Shinozaki, *Mater. Res. Express* **2**, 106001 (2015).
6. L. Kang, B. B. Jin, X. Y. Liu, X. Q. Jia, J. Chen, Z. M. Ji, W. W. Xu, P. H. Wu, S. B. Mi, A. Pimenov, Y. J. Wu, and B. G. Wang, *J. Appl. Phys.* **109**, 033908 (2011).
7. S. Ezaki, K. Makise, B. Shinozaki, T. Odo, T. Asano, H. Terai, T. Yamashita, S. Miki, and Z. Wang, *J. Phys.: Condens. Matter* **24**, 475702 (2012).
8. M. Chand, G. Saraswat, A. Kamlapure, M. Mondal, S. Kumar, J. Jesudasan, V. Bagwe, L. Benfatto, V. Tripathi, and P. Raychaudhuri, *Phys. Rev. B* **85**, 014508 (2012).
9. C. Carbillet, V. Cherkez, M. A. Skvortsov, M. V. Feigel'man, F. Debontridder, L. B. Ioffe, V. S. Stolyarov, K. Ilin, M. Siegel, C. Noûs, D. Roditchev, T. Cren, and C. Brun, *Phys. Rev. B* **102**, 024504 (2020).
10. B. Sacépé, C. Chapelier, T. I. Baturina, V. M. Vinokur, M. R. Baklanov, and M. Sanquer, *Phys. Rev. Lett.* **101**, 157006 (2008).
11. J. M. Graybeal and M. R. Beasley, *Phys. Rev. B* **29**, 4167 (1984).
12. D. Lotnyk, O. Onufriienko, T. Samuely, O. Shylenko, V. Komanický, P. Szabó, A. Feher, and P. Samuely, *Low Temp. Phys.* **43**, 919 (2017).
13. N. Ya. Fogel, E. I. Buchstab, A. S. Pokhila, A. I. Erenburg, and V. Langer, *Phys. Rev. B* **53**, 71 (1996).
14. A. Banerjee, L. J. Baker, A. Doye, M. Nord, R. M. Heath, K. Erotokritou, D. Bosworth, Z. H. Barber, I. MacLaren, and R. H. Hadfield, *Supercond. Sci. Technol.* **30**, 084010 (2017).
15. P. Szabó, T. Samuely, V. Hašková, J. Kačmarčík, M. Žemlička, M. Grajcar, J. G. Rodrigo, and P. Samuely, *Phys. Rev. B* **93**, 014505 (2016).
16. H. Raffy, R. B. Laibowitz, P. Chaudhari, and S. Maekawa, *Phys. Rev. B* **28**, 6607 (1983).
17. D. Shahar and Z. Ovadyahu, *Phys. Rev. B* **46**, 10917 (1992).
18. M. Strongin, R. S. Thompson, O. F. Kammerer, and J. E. Crow, *Phys. Rev. B* **1**, 1078 (1970).
19. D. B. Haviland, Y. Liu, and A. M. Goldman, *Phys. Rev. Lett.* **62**, 2180 (1989).
20. M. P. A. Fisher, *Phys. Rev. Lett.* **65**, 923 (1990).
21. V. F. Gantmakher and V. T. Dolgoplov, *Phys. Usp.* **53**, 1 (2010).
22. I. S. Burmistrov, I. V. Gornyi, and A. D. Mirlin, *Phys. Rev. B* **92**, 014506 (2015).
23. A. Kapitulnik, S. A. Kivelson, and B. Spivak, *Rev. Mod. Phys.* **91**, 011002 (2019).
24. B. Sacépé, M. Feigel'man, and T. M. Klapwijk, *Nat. Phys.* **16**, 734 (2020).
25. M. V. Feigel'man, A. I. Larkin, and M. A. Skvortsov, *Phys. Rev. Lett.* **86**, 1869 (2001).
26. M. V. Feigel'man, L. B. Ioffe, V. E. Kravtsov, and E. A. Yuzbashyan, *Phys. Rev. Lett.* **98**, 027001 (2007).
27. M. V. Feigel'man, L. B. Ioffe, V. E. Kravtsov, and E. Cuevas, *Ann. Phys.* **325**, 1390 (2010).
28. B. Sacépé, T. Dubouchet, C. Chapelier, M. Sanquer, M. Ovidia, D. Shahar, M. V. Feigel'man, and L. B. Ioffe, *Nat. Phys.* **7**, 239 (2011).
29. B. L. Al'tshuler and A. G. Aronov, *Sov. Phys. JETP* **50**, 968 (1979).
30. B. L. Altshuler and A. G. Aronov, *Electron–Electron Interaction in Disordered Systems*, Ed. by A. L. Efros and M. Pollak (North-Holland, Amsterdam, 1985).
31. P. W. Anderson, K. A. Muttalib, and T. V. Ramakrishnan, *Phys. Rev. B* **28**, 117 (1983).
32. H. Fukuyama, H. Ebisawa, and S. Maekawa, *J. Phys. Soc. Jpn.* **53**, 3560 (1984).
33. B. Rabatin and R. Hlubina, *Phys. Rev. B* **98**, 184519 (2018).
34. T. R. Kirkpatrick and D. Belitz, *Phys. Rev. B* **34**, 2168 (1986).
35. P. W. Adams, D. A. Browne, and M. A. Paalanen, *Phys. Rev. B* **45**, 8837 (1992).
36. A. M. Rudin, I. L. Aleiner, and L. I. Glazman, *Phys. Rev. B* **55**, 9322 (1997).
37. A. A. Koulakov, *Phys. Rev. B* **62**, 6858 (2000).
38. D. S. Antonenko and M. A. Skvortsov, *Phys. Rev. B* **101**, 064204 (2020).
39. B. Keck and A. Schmid, *J. Low Temp. Phys.* **24**, 611 (1976).
40. D. Belitz, *J. Phys. F: Met. Phys.* **15**, 2315 (1985).
41. D. Belitz, *Phys. Rev. B* **35**, 1636 (1987).
42. D. Belitz, *Phys. Rev. B* **35**, 1651 (1987).
43. D. Belitz, *Phys. Rev. B* **36**, 47 (1987).
44. A. M. Finkel'stein, *Phys. B (Amsterdam, Neth.)* **197**, 636 (1994).
45. S. Maekawa and H. Fukuyama, *J. Phys. Soc. Jpn.* **51**, 1380 (1982).
46. S. Maekawa and H. Fukuyama, *J. Phys. Soc. Jpn.* **52**, 1352 (1983).
47. Yu. N. Ovchinnikov, *Sov. Phys. JETP* **37**, 366 (1973).
48. H. Takagi and Y. Kuroda, *Solid State Commun.* **41**, 643 (1982).
49. H. Ebisawa, H. Fukuyama, and S. Maekawa, *J. Phys. Soc. Jpn.* **54**, 2257 (1985).
50. E. Abrahams, P. W. Anderson, D. C. Licciardello, and T. V. Ramakrishnan, *Phys. Rev. Lett.* **42**, 673 (1979).
51. L. P. Gorkov, A. I. Larkin, and D. E. Khmel'nitsky, *JETP Lett.* **30**, 228 (1979).
52. A. M. Finkel'stein, *JETP Lett.* **45**, 46 (1987).
53. M. V. Feigel'man and M. A. Skvortsov, *Phys. Rev. Lett.* **109**, 147002 (2012).



54. H. Kim, A. Ghimire, S. Jamali, T. K. Djidjou, J. M. Gerton, and A. Rogachev, *Phys. Rev. B* **86**, 024518 (2012).
55. K. B. Efetov, *Supersymmetry in Disorder and Chaos* (Cambridge Univ. Press, Cambridge, 1996).
56. A. M. Finkelstein, *Electron Liquid in Disordered Conductors*, Vol. 14 of *Soviet Scientific Reviews*, Ed. by I. M. Khalatnikov (Harwood Academic, Glasgow, 1990).
57. I. S. Burmistrov, *J. Exp. Theor. Phys.* **129**, 669 (2019).
58. F. Couedo, O. Crauste, L. Bergé, Y. Dolgorouky, C. Marrache-Kikuchi, and L. Dumoulin, *J. Phys.: Conf. Ser.* **400**, 022011 (2012).
59. Y. Ivry, C.-S. Kim, A. E. Dane, D. De Fazio, A. N. McCaughan, K. A. Sunter, Q. Zhao, and K. K. Berggren, *Phys. Rev. B* **90**, 214515 (2014).
60. C. Brun, T. Cren, V. Cherkez, F. Debontridder, S. Pons, D. Fokin, M. C. Tringides, S. Bozhko, L. B. Ioffe, B. L. Altshuler, and D. Roditchev, *Nat. Phys.* **10**, 444 (2014).
61. N. N. Bogoliubov, V. V. Tolmachev, and D. V. Shirkov, *A New Method in the Theory of Superconductivity* (Consultants Bureau, New York, 1959).
62. P. Morel and P. W. Anderson, *Phys. Rev.* **125**, 1263 (1962).
63. W. L. McMillan, *Phys. Rev.* **167**, 331 (1968).
64. P. W. Anderson, *Phys. Chem. Sol.* **11**, 26 (1959).
65. A. A. Abrikosov and L. P. Gor'kov, *Sov. Phys. JETP* **8**, 1090 (1959).
66. A. A. Abrikosov and L. P. Gor'kov, *Sov. Phys. JETP* **9**, 220 (1959).
67. S. Hikami, *Phys. Rev. B* **24**, 2671 (1981).
68. N. A. Stepanov and M. A. Skvortsov, *Phys. Rev. B* **97**, 144517 (2018).
69. B. A. van Tiggelen and S. E. Skipetrov, *Phys. Rev. E* **73**, 045601 (2006).
70. I. E. Smolyarenko and B. L. Altshuler, *Phys. Rev. B* **55**, 10451 (1997).
71. B. L. Altshuler and A. G. Aronov, *Solid State Commun.* **30**, 115 (1979).